U.P.B. Sci. Bull., Series D, Vol. 80, Iss. 3, 2018 ISSN 1454-2358

ANALYSIS OF HIGH POROSITY MICRO PERFORATED PANEL USING DIFFERENT METHODS

Marius DEACON[1], Grigore CICAN[2], Laurentiu CRISTEA[3], Luminita DRAGASANU[4]

Micro perforated panels (MPP) with low percent of opened area (POA) have been intensively studied using different methods, which determine the impedance of such structures. The present paper proposes a study regarding the most accurate and fastest method in impedance calculation of MPP with high POA. The proposed calculation methods are based on the Maa, Beranek, Transfer Matrix Method (TMM) and Finite Element Method (FEM). In FEM software the acoustic impedance of a MPP can be calculated using a simplified method that uses Maa equations and "Distance-Based Linearized Navier-Stokes-Fourier" (DBLNSF) method, that calculates the acoustic propagation in micro perforations taking into account the visco-thermal losses effects. All the proposed numerical results are compared with the impedance tube measurements performed on a micro perforated stainless steel sheet. The results highlighted that for MPP with high POA the DBLNSF method provides the most precise results followed by the Beranek empirical model. In conclusions are presented the advantages and the disadvantages of each of the calculation models and the comparison with the measurements results.

Keywords: MPP, acoustic simulation, acoustic impedance, porosity

1. Introduction

Micro perforated panel (MPP) is represented by a reactive structure used at noise control and noise reduction solution. Intensive studies [1-5] were made with perforated panel with a perforation rate, also named percent open area (POA), between 0.5% and 2% with perforation diameters between 0.3-1mm, which is placed at a certain distance from a hard-reflecting wall. The acoustic wave propagation through the panel lead to energy dissipation in heat, effect that

[1] Ph. D. Student, Faculty of Biotechnical Systems Engineering, University POLITEHNICA of Bucharest, e-mail: mariussdeaconu@gmail.com
[2] Lecturer, Faculty of Aerospace Engineering, University POLITEHNICA of Bucharest, Romania, e-mail: grigore.cican@upb.ro
[3] Ph. D. Student, Faculty of Biotechnical Systems Engineering, University POLITEHNICA of Bucharest, Faculty of ISB, e-mail: laurentiu_cristea@yahoo.com
[4] Ph. D. Student, Faculty of Biotechnical Systems Engineering, University POLITEHNICA of Bucharest, Faculty of ISB, e-mail: luminita.dragasanu@gmail.com

is produced by the viscous thermal losses from inside the perforation as the air molecules travel through the perforations, frictions losses occur, and this effect can be enhanced by reducing the diameter of the perforation. Intensive studies were conducted especially for widening the acting frequency domain. First studies related to the acoustic properties of the MPP were conducted by the Maa [6], afterwards the MPP being intensively researched resulting numerous patents, research paper and projects.

The effect of high POA was studied by Michael G Jones et al. [7] study that revealed that the acoustic resistance and reactance is decreasing with increasing of POA.

This paper proposes a design procedure for MPP by studying multiple methods to determine the fastest and precise method for modelling the MPP with high POA. The numerical results will be compared with the experimental measurements performed with the impedance tube.

2. The principles and mathematical models

A micro perforate panel with a thickness *t*, perforation diameter *d*, holes step *b* and air cavity length *D* is presented in Fig 1. Only the plane wave at normal incidence on the perforated panel is considered in this study. The numerical methods described by the Maa [6], Beranek [8], Transfer Matrix Method TMM [9] and two FEM methods are proposed and compared in this paper.

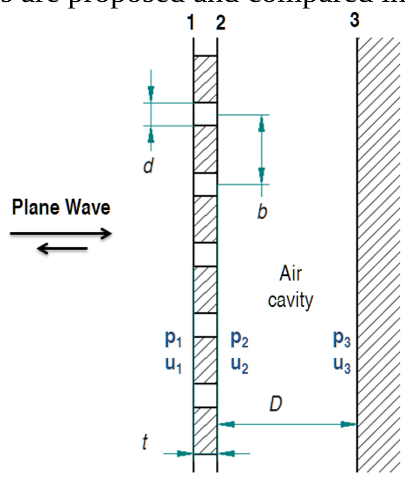

Fig. 1. Schematic representation of a MPP

Considering that the solid has no motion, only the acoustic transfer across the sheet is considered. The impedance Z_p of a single perforation can be written as [10]:

$$Z_p = \frac{\partial p}{\bar{u}} = R_p + jX_p \tag{1}$$

where $\partial p = p_2 - p_1$ is the pressure drop across the panel and considering $u_1 = u_2$ the $\bar{u}$ is the average normal particle velocity across the perforation, R_p is the acoustic resistance, X_p is the acoustic reactance. From the above assumptions, the normalized specific acoustic impedance is:

$$z_p = \frac{Z_p}{\rho_0 c_0} = r_p + jx_p \tag{2}$$

where ρ_0 is the density of the medium at rest (1.225 kg/m^3 for the air at ambient conditions) and c_0 the speed of sound at rest (340 m/s for the air at ambient conditions).

The transfer impedance of a multi-perforated panel is expressed in relation to the porosity of the plate (also called open area) σ, which is defined as the ratio of open area by the total surface of the plate. For a square grid, POA is defined as $\sigma = \pi \frac{a^2}{b^2}$ and for triangular grid, the POA is $\sigma = \frac{2\pi a^2}{\sqrt{3}d^2}$ [10].

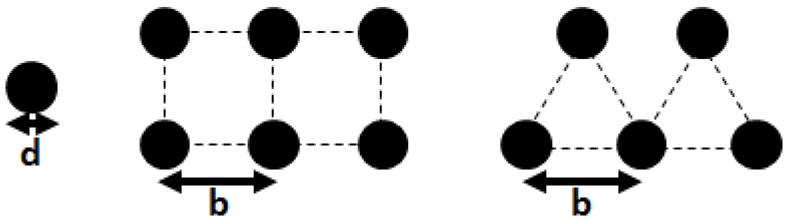

Fig. 2. Square and triangular perforation grid

The transfer impedance and dimensionless transfer impedance of the whole plate are:

$$\bar{Z}_p = \frac{Z_p}{\sigma} = \frac{1}{\sigma}\left(R_p + jX_p\right) \tag{3}$$

$$\bar{z}_p = \frac{1}{\sigma}\left(r_p + jx_p\right) \tag{4}$$

Maa models. First studies related by the impedance of short tube and sound propagation through thin cylindrical perforation in a panel were performed by Crandall after Rayleigh [11]. The acoustic impedance of a tube was approximated by Maa [6] after Crandall's solution for the wave equation. The exact formula for the specific acoustic impedance of an MPP proposed by Maa [6], which includes the impedance of the tube, given by Crandall and the end correction, is:

$$Z_{Maa\_exact} = \frac{\sqrt{2}\mu s}{\sigma d} + \frac{j\omega\rho_0}{\sigma}\left\{0.85d + t\left[1 - \frac{2}{s\sqrt{-j}}\frac{J_1\left(s\sqrt{-j}\right)}{J_0\left(s\sqrt{-j}\right)}\right]^{-1}\right\} \tag{5}$$

The second approach that will be analysed is the approximate formula proposed by Maa [6], which includes the impedance of the tube and the end corrections:

$$Z_{Maa\_approximate} = \frac{32\mu t}{\sigma d^2}\left(\sqrt{1+\frac{s^2}{32}} + \frac{\sqrt{2}sd}{32t}\right) + \frac{j\omega t\rho_0}{\sigma}\left(1 + \frac{1}{\sqrt{3^2+\frac{s}{2}}} + 0.85\frac{d}{t}\right) \tag{6}$$

After the impedance of the micro perforation is calculated, the total impedance must be determined taking into account the impedance of the back air cavity from which results the total impedance of the structure:

$$\begin{aligned} Z_{back\_air} &= -i\rho_0 c_0 \cot(kD) \\ Z_{total} &= Z_{M(MPP)} + Z_{back\_air} \end{aligned} \tag{7}$$

where k is the wave number and D is the cavity length. From the total impedance of the system, the acoustic reflection coefficient and acoustic absorption coefficient at normal incidence are determined according to following equations:

$$R = \frac{(Z_{total} - \rho_0 c_0)}{(Z_{total} + \rho_0 c_0)} \tag{8}$$

$$\alpha = 1 - |R|^2 \tag{9}$$

Beranek model. In their study, Beranek and Ver [8] used an empirical model for calculating the acoustic resistance and reactance of a perforated panel.

$$R_{pB} = \frac{8.076\times 10^{-5}\sqrt{f}}{\sigma}\left(1+\frac{t}{d}\right)$$
$$X_{pB} = 0.0185\,\frac{f}{\sigma}\left[\frac{0.0044}{\sqrt{f}}\left(1+\frac{t}{d}\right)+t+\delta\right] \tag{10}$$

where R_{pB} and X_{pB} is the resistance and reactance part, $\delta = 0.85 d\varphi(\sigma)$ is a function of the porosity and $\varphi(\sigma) = 1 - 1.47\sqrt{\sigma} + 0.47\sqrt{\sigma^3}$.

The end correction term is represented by the 0.85 constant from the reactance. To determine the absorption, the impedance of the back air cavity is added from eq.7 and the absorption is determined according eq. 9.

Transfer Matrix Method (TMM) is a practical way in finding the acoustic impedance of different structures [5]. In addition, this method is a very practical way to determine the acoustic impedance of a complex structure [12]. The TMM consist in modelling the panel as a four-pole matrix, which includes the sound pressure and particle velocity on each side of the MPP. In fig. 1 at the top face of the perforated panel, we have the pressure and velocity p_1 and u_1 where at the other surface we have the pressure p_2 and velocity u_2. The transfer matrix can be expressed as:

$$\begin{bmatrix} p_1 \\ u_1 \end{bmatrix} = \begin{bmatrix} A & B \\ C & D \end{bmatrix} \begin{bmatrix} p_2 \\ u_2 \end{bmatrix} \tag{11}$$

in which the A, B, C, D are the four pole parameter of the acoustical element. Considering the third element, a hard reflecting wall, the particle velocity u_3 at surface is zero.

The total impedance of the acoustic structure presented in Fig 1 is resulted from the multiplication of the matrix of the panel with the matrix of the back air cavity:

$$T = T_{MPP} * T_{aer} = \begin{bmatrix} 1 & Z_T \\ 0 & 1 \end{bmatrix} * \begin{bmatrix} \cos(kD) & j\rho_0 c \sin(kD) \\ j\,\dfrac{\sin(kD)}{\rho_0 c} & \cos(kD) \end{bmatrix} \tag{12}$$

Z_T is the acoustic impedance of the perforated panel calculated from the eq. 6, D is the cavity length and k is the wavenumber. The input impedance of a MPP system is obtained from the relation:

$$Z_{TMM} = \frac{T(1,1)}{T(2,1)} \tag{13}$$

in which *T(1,1)* and *T(2,1)* represents the first and second element of the total impedance matrix. The acoustic reflection coefficient is obtained by introducing Z_{TMM} in eq.8, from which the acoustic absorption coefficient is determined from the eq.9.

3. Finite element methods

The MPP can be computed using FEM to determine the impedance at normal incidence, using MSC Actran software. In the FEM software, the MPP can be modelled in two ways.

The first way is to use a built in module of the software, which uses the exact solution according to Maa [6]. This module reduces the model dimensions by pre-calculating the total impedance of the perforated panel both with the back air cavity. The resulted impedance is assigned only to a surface of the CAD model without meshing the fluid from perforations and the back air cavity.

The second method to determine the acoustic impedance of an MPP is to model and mesh the fluid inside the perforation as a visco-thermal component using a DBLNSF model "Distance-Based Linearized Navier-Stokes-Fourier" [10]. In this paper, the both methods are considered and compared.

For the first FEM method with Maa equations (5), the model consists only in the air from the impedance tube as is presented in Fig 3. A reduced CAD model was used to reduce the computational time, where the diameter of the impedance tube was 5mm with the length of 60mm. The red surface represents the surface for which the impedance was computed using the Maa equation. The blue region represents the boundary condition of the acoustic radiating surface with plane waves, for which an intensity of 1W in the sample direction was defined. Also on the same surface, a free field condition in the opposite direction was imposed in order to compute the reflected wave, which is reflected by the sample. The remaining non-defined surfaces are considered by the software as hard walls with total reflection. The air properties from the all domain were ρ_0=1.225 kg/m^3, c=340m/s and air dynamic viscosity 18.2e+06 Pa.s. The parameters of the perforated panel studied in the FEM analysis were: perforation diameter *d*=5e-04m, thickness *t*=5e-04 m, holes step *b*=1.5e-03 m from which results a porosity of σ=8.73%. Two different back air cavity lengths were modelled and studied: $D_{1,2}$=0.02 and 0.04 m. It is important that in FEM analyses the motion of the solid part was not considered, only the acoustic transfer across the sheet being considered. The analysis was defined in the 50-7000Hz frequency domain with a frequency step of 10Hz. As a rule in mesh definition, when quadrilateral elements are used in acoustic analysis, four elements per wavelength must be created for the highest studied frequency. In our case, considering the small dimensions of the virtual impedance tube, sub-millimetre elements were used. To determine the acoustic absorption coefficient at normal incidence, the radiated power of the noise source surface in the direction of the sample and the power of the reflected wave were used in the next equation:

$$\alpha = \frac{\left(P_{incident} - P_{reflected}\right)}{P_{incident}} \tag{14}$$

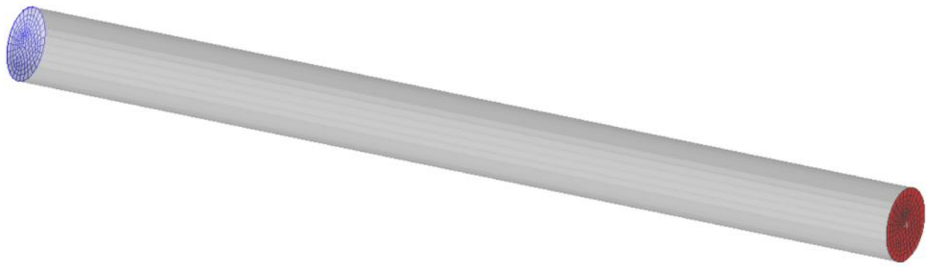

Fig. 3. Grid of impedance tube fluid – first FEM method

In the second FEM method, a DBLNSF method was used, where the mesh needs to be sufficiently refined close to the wall to capture accurately the boundary layer effects. A major drawback of the proposed model is the mesh refinement conditions, which can drastically increase the computational time. Therefore, only one perforation was chosen together with the air volume from the cavity that corresponds to it, according to the Fig. 4. The hexagonal volume represents the back air cavity, the cylindrical shape represents the fluid from the impedance tube and the red surface represents the boundary condition of plane wave. As it is presented in detail of Fig. 4, the element size in the perforation area was limited at 5.04e-05 m and in FEM analysis, this volume was defined as visco-thermal component, to model the acoustic propagation in narrow channels, which computes the visco-thermal losses. The elements length from other fluid domains was set in order to respect the rule of eight tetrahedral elements per the minimum wavelength. As in the first FEM model, the motion of the solid part was not considered, the solid being subtracted from the model as is presented in Fig. 4.

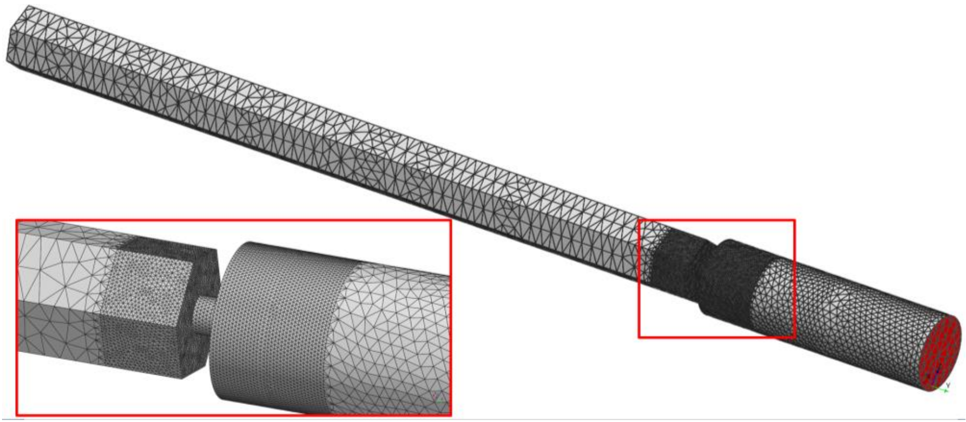

Fig. 4. Grids of impedance tube, microperforation chanel and cavity fluid – second FEM method

The air properties from the all domain were: ρ_0=1.225 kg/m^3, c=340m/s, air dynamic viscosity 18.2e+06 Pa.s, and the same plane wave condition was applied as in the first model case.

4. Impedance tube measurements

The measurements of acoustic absorption coefficient at normal incidence were made by using a 28mm diameter impedance tube and two microphones. The method uses transfer function between the both signals according to the ISO 10534-2 [13]. The sample is represented by a stainless steel sheet with diameter of 28mm, with perforations diameter *d*=5e-04m, sheet thickness *t*=5e-04 m, distance between perforations *b*=1.5e-03 m, resulting a porosity of σ=8.73%. Two different back air cavity lengths were measured $D_{1,2}$=0.02 and 0.04 m. The tested sample and the impedance tube are presented in the Fig. 5. The image on the right presents the impedance tube and the microphones position.

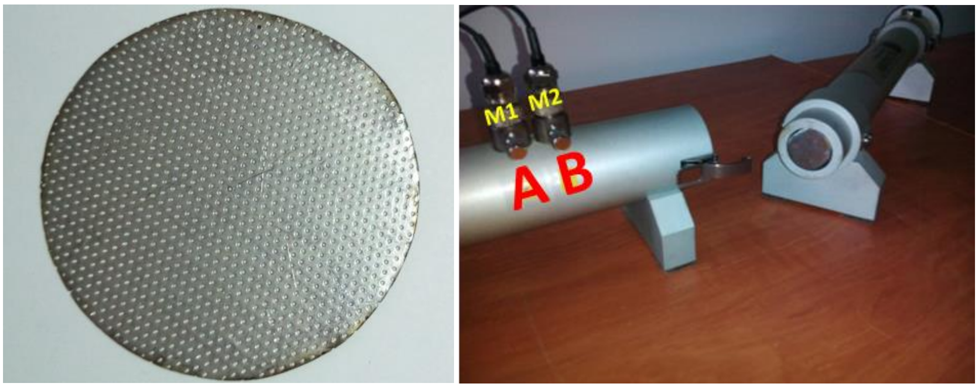

Fig. 5. Impedance tube and steel micro perforated plate

According to the ISO 10534-2, the acoustic absorption coefficient is obtained by using two microphones (M1, M2) positioned at a distance from the sample. The standard position is with microphone M1 in position A and M2 in position B, from which the uncorrected transfer function between them H^{I}_{12} is measured. In order to increase the precision of the measurements, the standard provides phase and amplitude calibration, technique that consists in microphones interchange. The second uncorrected transfer function is measured by placing microphone M1 in position B and the microphone M2 is placed in position A. Using the two transfer functions, the corrected transfer function is obtained:

$$H_{12}(\omega) = \sqrt{H^{I}_{12}(\omega) * H^{II}_{12}(\omega)} \tag{15}$$

The acoustic reflection coefficient $R(\omega)$ is determined by using the corrected transfer function:

$$R(\omega) = \frac{e^{-jk_0 s} - H_{12}(\omega)}{H_{12}(\omega) - e^{jk_0 s}} e^{2jk_0 x_1} \tag{16}$$

in which s represents the distance between the microphones, x_1 the distance from the sample to the M1 in standard position and k_0 is the wavenumber.

The acoustic absorption coefficient at normal incidence is determined from the reflection coefficient:

$$\alpha = 1 - |R(\omega)|^2 \tag{17}$$

5. Results

In this paragraph, the results of the above models are compared with the measurement results obtained on the impedance tube. From this comparison on panels with high POA, it is expected to observe if the models give close results and which one gives the closest result to the ones obtained by measurement.

The study is focusing on one type of micro perforated panel from stainless steel with: round perforation of d=5e-04m diameters, thickness t=5e-04m, holes step b=1.5e-03 m, resulting a porosity of σ=8.73% and two different cavity deeps D=0.02 m and 0.04m.

The comparison of the acoustic absorption coefficient at normal incidence for a cavity deep D=0.02 m is presented in the Fig. 6.

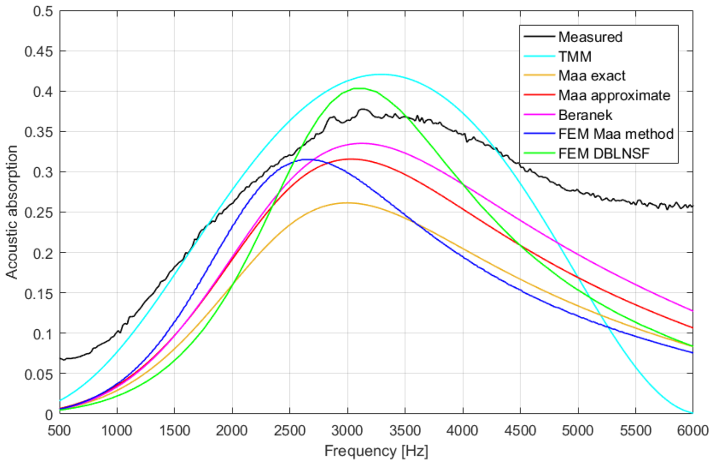

Fig. 6. Comparison of the models and experimental results for air cavity length of 0.02 m

It can be seen that for high porosity panel, both Maa model and FEM model with Maa method, provide inaccurate data in comparison to the measurement. Beranek model, FEM with DBLNSF model and TMM model provided close results with the measurement, FEM providing the closest results at the main absorption frequency. In addition, the Beranek model and TMM tends to have a broadband spectrum like the measurement results. In the second case, Fig. 7, with the cavity deep of D=0.04 m, it can observed that the FEM DBLNS method provided the closest results to the measurement, especially at the second maxima coefficient at 5500Hz.

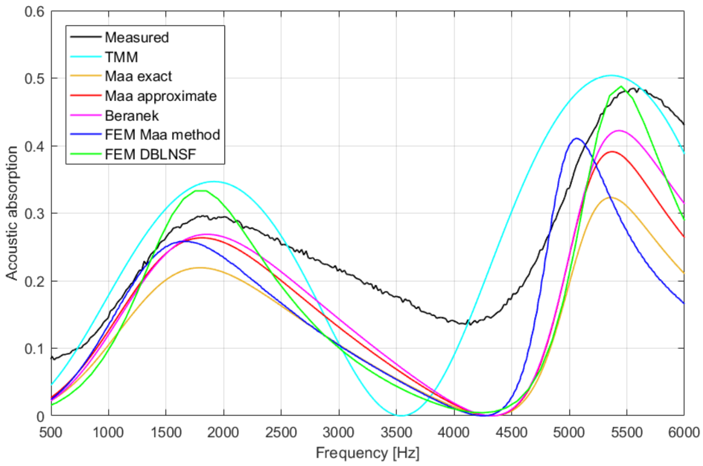

Fig. 7. Comparison of the model and experimental results for air cavity length of 0.04 m

As in the first case the Beranek model obtained good results at the two absorption maxima, both in terms of absorption and frequency. Also the TMM method obtained close results on both maxima and also as spectrum profile. The deviation of measurements on the frequency domain ends can be caused by the stiffness of the sample fixture and also from the interaction of the air flow perturbation between the perforations. Fig. 8 highlights the acoustic pressure and particle velocity in the neck of the microperforation, where the top domain is the fluid from the impedance tube and at the buttom is a portion of the air cavity. As is defined in eq.1, the impedance of a perforation is expressed in relation with the pressure difference from both ends of the perforation, where in our case the pressure difference at 1750Hz is almost 10Pa.

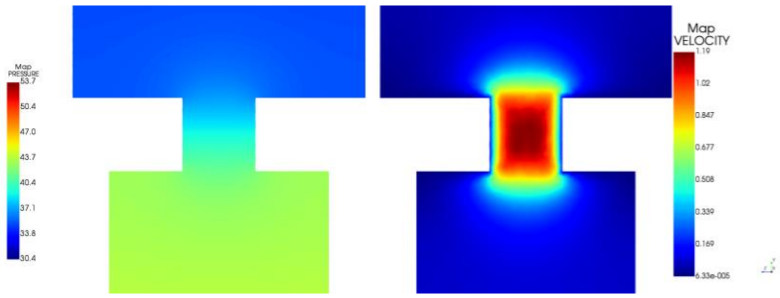

Fig. 8. FEM results at 1750Hz for cavity length of 0.04 m (left: pressure, right: velocity)

From Fig. 9, from velocity plot, it can be seen that the flow around the perforation is distorted, affecting the viscous boundary layer. The pressure difference is higher than at 1750Hz and due to viscous boundary layer distortion, the impandance is growing, resulting an acoustic energy dissipation in the perforation neck.

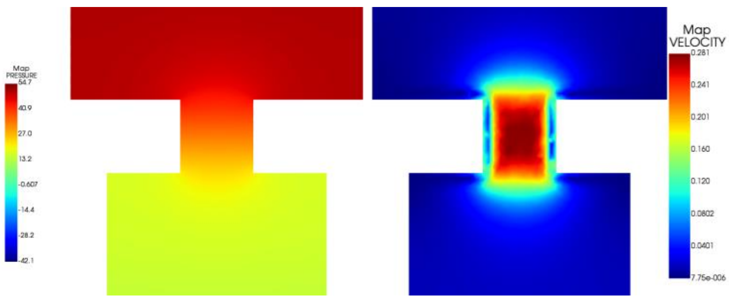

Fig. 9. FEM results at 5450Hz for cavity length of 0.04 m (left: pressure, right: velocity)

6. Conclusions

Many studies were made on micro perforated panel with porosity lower than 3%, which provides sufficient resistance to dissipate the acoustic energy in heat. Finding on market MPP with low porosity can be a problem but a solution is to use existing MPP with high POA. The aim of this study was to compare several models from the literature, to see which one provide the closest results to the impedance tube measurement. The FEM DBLNSF model results can be declared the most precise method. The main advantage is given by the possibility to determine the impedance even for complex perforation shapes or non-uniformly distributed perforations, but the major disadvantage is represented by the long computing time. Small elements must be used in the area of the viscous and thermal boundary layer, to observe better the visco-thermal effects and to increase the precission of the computation. Comparing the results of TMM with the Beranek model, from the point of view of absorption maxima and their frequencies, the second model can be considered more precisely. Taking into account the simplicity of the Beranek model, this can be chosen as the optimum model in impedance calculation of the MPP with high POA.

In the next researches, it is intended to raise the acoustic resistance of high POA MPP by using metallic micromesh and to study the influence on the acoustic impedance by decreasing the air density from the cavity, which can be conducted by creating a semi vacuum condition.

R E F E R E N C E S

[1]. *D. Herrin, X. Hua, and J. Liu*, Microperforated panel absorber design: a tutorial, The 21st International Congress on Sound and Vibration, 13-17 July, 2014, Beijing, China

[2]. *D. Herrin* and *J. Liu*, Properties and Applications of Microperforated Panels, sound & Vibration, 45(7):6-9, July 2011.

[3]. *K. Sakagami, M. Morimoto and M. Yairi*, Recent developments in applications of microperforated panel absorbers, ICSV14, July 2007, Cairns, Australia.

[4]. *S. Allam and M. Åbom*, Experimental Characterization of Acoustic Liners with extended reaction, 14th AIAA/CEAS Aeroacoustics Conference, May 2008, Vancouver, Canada.

[5]. *S. S. Jung, Y. T. Kim and D. H. Lee*, Sound Absorption of Micro-Perforated Panel, Journal of the Korean Physical Society, **Vol. 50**, No. 4, April 2007, pp. 1044-1051.

[6]. *D. Y. Maa*, Potential of microperforated panel absorber, Journal of the Acoustical Society of America, 104(5):2861–2866, 1998

[7]. *M. G. Jones, M. B. Tracy, W. R. Watson and T. L. Parrott*, Effects of liner geometry on acoustic impedance, 8th AIAA/CEAS Aeroacoustics Conference & Exhibit Breckenridge, Colorado.

[8]. *L. L. Beranek and I. L. Ver*, Noise and Vibration Control, Engineering (John Wiley and Sons, New York, 1992), Chap. 8.

[9]. *Z. Tao, B. Zhang, D. Herrin and A. Seybert*, Prediction of Sound-Absorbing Performance of Micro-Perforated Panels using the Transfer Matrix Method, 05NVC-339

[10]. ***Actran 17.1 User’s Guide, Volume 1 Installation, Operations, Theory and Utilities

[11]. *I. B. Crandall*, Theory of Vibration System and Sound, New York, 1926, pp. 229.

[12]. *L. Dengke, C. Daoqing, L. Bilong and J. Tian*, Improving sound absorption bandwidth of micro-perforated panel by adding porous materials, Inter-noise 2014.

[13]. SR EN ISO 10534-2 Acoustics, Determination of sound absorption coefficient and impedance in impedance tubes, Part 2: Transfer-function method.